*forests*

MDPI

*Article*

# Genotypic and Silvicultural Controls on Wind Damage, Failure Mode, and Productivity in a Radiata Pine Trial Following Cyclone Gabrielle

**Michael S. Watt [1,*], Kate Halstead [2,*], Tommaso Locatelli [2], Nicolò Camarretta [3], Sadeepa Jayathunga [3] and Juan C. Suárez [2]**

[1] Bioeconomy Science Institute, Tuhiraki, 19 Ellesmere Junction Road, Lincoln 7608, New Zealand
[2] Forest Research, Northern Research Station, Bush Estate, Roslin, Scotland EH25 9SY, UK; tom.locatelli@forestresearch.gov.uk (T.L.); juan.suarez@forestresearch.gov.uk (J.C.S.)
[3] Bioeconomy Science Institute, Titokorangi Drive, Private Bag 3020, Rotorua 3046, New Zealand; nicolo.camarretta@scionresearch.com (N.C.); sadeepa.jayathunga@scionresearch.com (S.J.)
* Correspondence: michael.watt@scionresearch.com (M.S.W.); kate.halstead@forestresearch.gov.uk (K.H.)

**Abstract**

Storm damage poses an increasing risk to radiata pine (*Pinus radiata* D. Don) plantations in New Zealand as extreme wind events intensify under climate change. This study quantified wind damage following ex-tropical Cyclone Gabrielle in a seven-year-old genetics trial comprising 12 genotypes grown under four stand configurations defined by contrasting stocking (833 and 1282 stems/ha) and cultivation (with and without cultivation) treatments. The genotypes comprised a *Pinus attenuata* × *P. radiata* var. *cedrosensis* hybrid, ten anonymised radiata pine clones and an industry-standard radiata pine seedlot. Field assessments and unmanned aerial vehicle UAV laser scanning were used to classify damage into stem breakage and overturning and to derive structural metrics, including tree diameter, height, slenderness, volume, crown width and crown volume. Overall, 16.7% of trees were damaged, with stem breakage (10.2%) occurring more frequently than overturning (6.5%). Averaged across the four treatments, total damage significantly ranged from 10.4% in the high stocking cultivated treatment to 23.5% in the low stocking no cultivation treatment. Variation between the 12 genotypes was highly significant, with breakage, overturning and total damage ranging from 3.3%–25.4%, 1.4%–15.0% and 6.6%–29.5%, respectively, between the 12 genotypes. Two radiata pine clones with high growth rates and low to moderate wind damage had the highest post-storm total stem volume per hectare, which greatly exceeded that of the hybrid or the widely planted radiata pine seedlot. These findings highlight the potential of clones that combine high growth rates and resistance to wind damage to maintain high productivity under a changing climate with a greater frequency of extreme weather events.

**Keywords:** Cyclone Gabrielle; drone; ex-tropical cyclone; genotype; LiDAR; radiata pine; UAV; wind risk

Check for updates

Academic Editor: Aleksandar Dj Valjarević

Received: 8 January 2026
Revised: 12 February 2026
Accepted: 13 February 2026
Published: 17 February 2026

**Copyright:** © 2026 by the authors. Licensee MDPI, Basel, Switzerland. This article is an open access article distributed under the terms and conditions of the Creative Commons Attribution (CC BY) license.

## 1. Introduction

Extreme weather events are projected to increase in both frequency and severity over the course of this century as a consequence of rising mean annual air temperatures driven by climate change [1]. These events pose substantial challenges worldwide, and New Zealand is no exception. In recent years, the country has experienced several episodes of

extraordinary weather, including the devastating impacts of ex-tropical Cyclone Gabrielle, which struck the north-eastern regions of the North Island during February 2023 [2]. The cyclone triggered over 800,000 landslides [3], caused widespread forest windthrow, inundated low-lying areas through severe flooding, and inflicted extensive damage on critical infrastructure. Collectively, these impacts resulted in billions of dollars in recovery costs.

Cyclone Gabrielle produced exceptional rainfall along the east coast of New Zealand, with several locations receiving more than 300 mm in 24 h and peak daily totals exceeding previous historical records [4]. Attribution analyses show that anthropogenic warming increased the intensity of Gabrielle's extreme rainfall by approximately 20%–30% [4]. In a broader hazard context, Gabrielle's rainfall footprint is consistent with a present-day 1-in-100 to 1-in-250-year design storm for New Zealand, and storms of similar magnitude are projected to become substantially more likely under continued warming [5]. The scale and intensity of this event highlighted New Zealand's growing vulnerability to extreme climatic disturbances.

The New Zealand forestry sector is particularly exposed to these risks, as 90% of the plantation estate comprises radiata pine (*Pinus radiata* D. Don) [6], which is prone to wind damage [2,7,8]. In New Zealand radiata pine forests, storm damage commonly occurs through both stem breakage and overturning, with uprooting more frequently associated with wetter, shallower soils and older stands, and stem breakage relatively more common in younger or mid-rotation stands on better-drained sites [9,10]. Resistance to stem breakage is closely associated with stem diameter and wood properties, whereas resistance to uprooting has been empirically related to tree size and leverage, commonly expressed as height $\times$ diameter$^2$ or the height:DBH ratio [11–13]. The tree slenderness coefficient (TSC) is therefore often expected to be positively associated with wind damage in older structurally mature forests [14–16].

During severe storm events, these failure mechanisms can lead to damage at both the individual-tree and stand scales, resulting in substantial economic losses and long-term ecological consequences [10]. Such damage reduces forest productivity, compromises timber quality and market value, increases susceptibility to pests and diseases, and disrupts stand-level carbon sequestration, undermining both short-term profitability and long-term sustainability [11]. These impacts highlight the urgent need for robust approaches to predict wind risk and implement management practices aimed at mitigating damage before it occurs [17].

Despite the economic and ecological importance of wind resilience, significant knowledge gaps remain. In particular, the responses of different radiata pine hybrids and genotypes to wind stress are not yet fully understood, and the influence of key silvicultural practices, such as crop stocking levels (also known as stand density), thinning intensity, and pruning regimes, on wind damage incidence are still uncertain [18]. Addressing these gaps is essential for strengthening the resilience of plantation forestry, especially as climate-driven storm risks continue to escalate. Accordingly, this study characterises patterns of wind damage observed in a radiata pine genetics trial located in the central North Island of New Zealand following ex-tropical Cyclone Gabrielle in February 2023. The trial includes 11 radiata pine genotypes and a radiata pine hybrid (termed genotypes, hereafter) replicated across four treatments combining initial stocking (833 vs. 1282 stems/ha) and establishment practice (cultivated vs. non-cultivated).

This paper aims to characterise the impacts of the cyclone on the trial by (i) quantifying the incidence and severity of different damage modes (principally stem breakage and overturning) across the four stand treatments; (ii) evaluating variation between the 12 individual genotypes in overall damage susceptibility and in their tendency for particular damage modes; and (iii) characterising the relationships between tree structural

attributes, such as tree size, slenderness, and crown form, and damage occurrence and type; and (iv) determining the impacts of the cyclone on overall productivity between genotypes and treatments. The findings are intended to inform the selection of more wind-resilient genotypes and the refinement of establishment and silvicultural practices that reduce storm-related losses in similar plantation forests.

## 2. Materials and Methods

### *2.1. Study Site and Treatment Layout*

The study site, which is located in the central North Island (latitude −39.09°, longitude 175.83°) at 544 m elevation (Figure 1), has a mean air annual temperature of 10.7 °C, and annual rainfall of 2038 mm. The soil is classified as a Typic Orthic Pumice soil in the New Zealand Classification System [19], corresponding to a Humic Ustivitrands [20], which is derived from volcanic air fall deposits from the Taupo volcanic centre (1860 ± 100 BP) [21]. The soil is well drained sandy loam, with a sub-soil horizon of very gravelly (pumice gravels) soils, with no barriers to rooting depth for at least 1 m. The site was a moderately improved pasture before trees were established in 2016. The trial is part of a series of six trials established across New Zealand between 2015 and 2018, with the purpose of exploring current and future limitations to wood productivity through management practices [22].

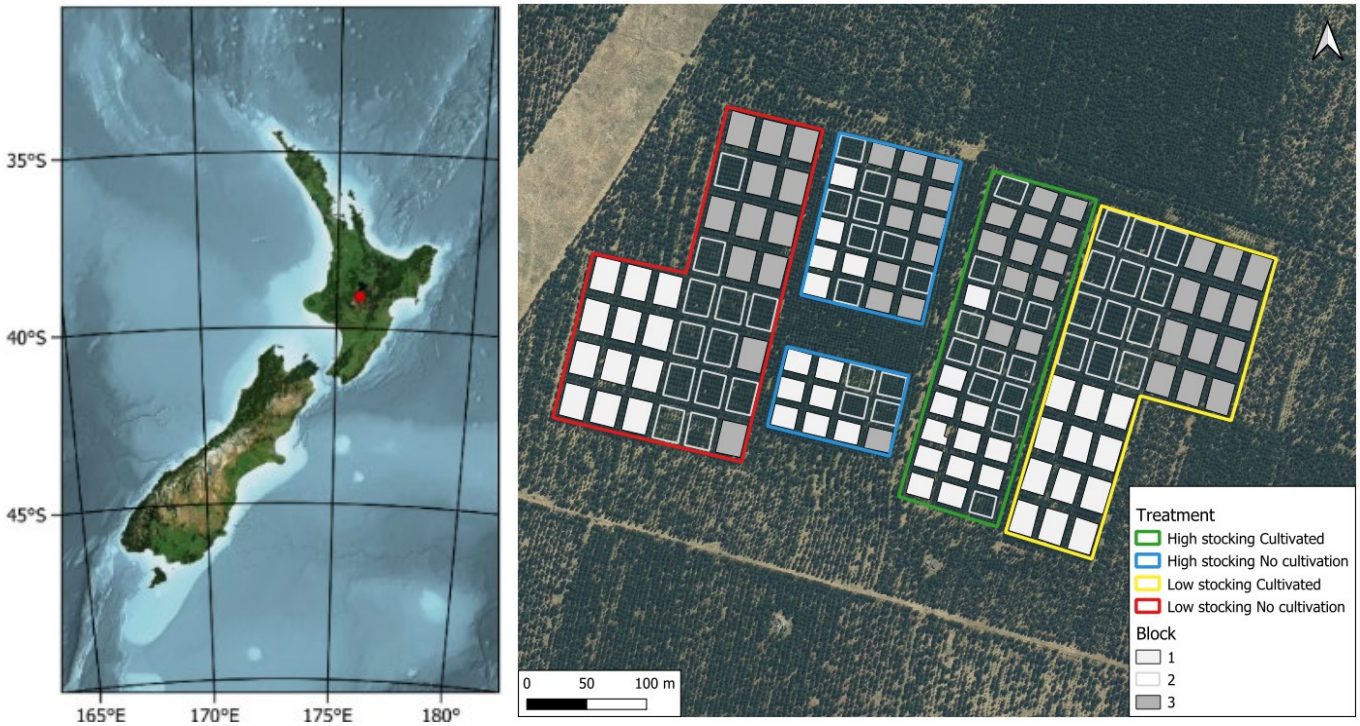



**Figure 1.** Maps showing (**Left**) location of the study site (red dot) within New Zealand, and (**Right**) the layout of the four treatments and three genotype blocks, within each treatment, at the trial site.

The four treatments at the site consisted of two initial stockings and two pre-afforestation site preparation methods (cultivation). The trial was established at two crop stockings that included 833 and 1282 stems/ha. Cultivation was undertaken at two levels that included either no cultivation, or cultivation using a disc implement to form raised soil ridges between furrows through disrupting the grass thatch. Cultivation represented the standard operational practice for this site. These two cultivation treatments were combined with the two initial stockings to produce four distinct areas with the factorial combination of stocking and cultivation (Figure 1). This design provides a unique opportunity to examine how stand structure and genetic variation interact to influence storm damage outcomes.

Twelve distinct radiata pine genotypes were planted at the study site following the cultivation treatment. These comprised a commercially important *Pinus attenuata* × *P. radiata* var. *cedrosensis* hybrid (genotype 1), ten commercially deployed radiata pine clones (genotypes 2–11, inclusive) and an industry-standard radiata pine seedlot (genotype 12). The standard industry seedlot was GF19 with this symbol designating growth (G) and form (F) on the GF rating scale [23]. As the identity of the clonal material is commercially sensitive these 10 clones were anonymised with a number from 2 to 11.

Trees were established in plots of 81 individuals following a 9 × 9 grid, with the central 7 × 7 grid of trees used to collect ongoing data. The outer two rows served as buffer trees to minimise edge effects. Each plot included a single genotype, and the twelve genotypes were randomly allocated within a block, with three replicate blocks established within each of the four treatment areas (Figure 1). Although the blocks were generally spatially clustered, they were not always strictly contiguous. In total, 144 plots were created (12 genotypes × 4 treatments × 3 blocks), covering an area of 13.4 ha. At the time of the cyclone (peak local intensity: 12–13 February 2023), the trees were seven years old. As no pruning or thinning had been undertaken, and survival rates were very high the stocking immediately prior to the cyclone, remained close to their original planting levels of 833 and 1282 stems $ha^{-1}$.

### 2.2. Field Measurements

Pre-cyclone measurements were undertaken between 9 and 22 of August 2022. Measurements comprised diameter at breast height (DBH) and tree status (alive or dead) for all trees. Using an unmanned aerial vehicle (UAV), tree height was determined from Light Detection and Ranging (LiDAR) data (see Section 2.3). During this assessment 7005 trees were alive which constituted a very high overall survival rate of 99.3%.

Cyclone Gabrielle occurred on the 12 and 13 of February 2023. Post-cyclone field measurements, undertaken between 23 September and 1 October 2024 across all 144 plots, were used to assess cyclone-related impacts. Although damage was assessed 19 months after the cyclone, this delay was unlikely to significantly affect documented damage, as (i) the main failure types (stem breakage and overturning) are persistent and readily identifiable in the field, and (ii) there were no significant storms following Cyclone Gabrielle and the site was not cleaned up prior to post-storm measurements. During this assessment, DBH and survival were re-evaluated for all trees, and wind damage was classified for each tree. As with pre-cyclone measurements, tree height was determined using UAV LiDAR (see Section 2.3).

Damage assessments were undertaken both pre- and post-cyclone at the same time as the measurements. Standard tree description codes were used to identify stem defects, which in this study focussed on whether trees had stem breakage or were overturned (Figure 2). Of the 7005 trees measured in 2022, 36 trees were excluded from analyses as stem breakage for these trees were recorded prior to the cyclone. An additional seven trees were also excluded as debris obstructed post-cyclone measurements. Following these exclusions, there were 6962 trees available to investigate the impacts of Cyclone Gabrielle on the trial.



**Figure 2.** Damage within the stand, showing (**Left**) toppled tree and (**Right**) close up of the root system.

### 2.3. Remote Sensing Data Collection

Using a UAV, very high-resolution imagery and laser scanning data were collected over the site, prior to the cyclone on 17 October 2022 (Figure 3). RGB imagery was acquired by UAV using the DJI Zenmuse P1 sensor (DJI, Shenzhen, China). UAV LiDAR was captured utilising the LidarUSA Snoopy V-series laser scanning system (LiDAR USA, Hartselle, AL, USA), which included an integrated Riegl MiniVUX-1 sensor (RIEGL Laser Measurement Systems GmbH, Horn, Austria) mounted on a DJI Matrice 600 Pro (DJI, Shenzhen, China). The UAV LiDAR capture was conducted at an altitude of 45 m above the ground, and at a speed of 5 m/s achieving a point density of approximately 1025 points/$m^2$. The RGB data was used to generate orthomosaics with a resolution of 1.34 cm.

Data co-registration using ground control points was carried out to ensure the precise alignment of the pre- and post-cyclone datasets. Following co-registration, the UAV LiDAR data was pre-processed following standard steps, which included denoising, ground classification, and ground normalisation, using the LASTools software package version 241106 [24]. Canopy height models (CHM) were generated for both time stamps at a 10 cm spatial resolution.

Individual tree detection within the CHMs was achieved through a local maxima-based method, implemented using the lidR package [25] in R software version 4.4.3 [26]. The automatically detected tree peak locations were then visually inspected and rectified in case of inaccuracies. The remote sensing detected tree peak locations were linked with a plot and tree ID database, for further analysis and ground truthing.

Next, tree crown delineation was performed on the pre-cyclone CHM using a marker-controlled watershed method, with verified tree peaks used as seed points. The resulting crowns were then used to segment the pre-cyclone LiDAR point cloud into individual tree segments. From each individual tree segment, tree height, crown width, and crown volume were extracted and linked to tree-level identifiers. Crown width was calculated from the horizontal extent of the crown, and crown volume was calculated as the volume enclosed by a three-dimensional convex hull fitted to the crown point cloud.

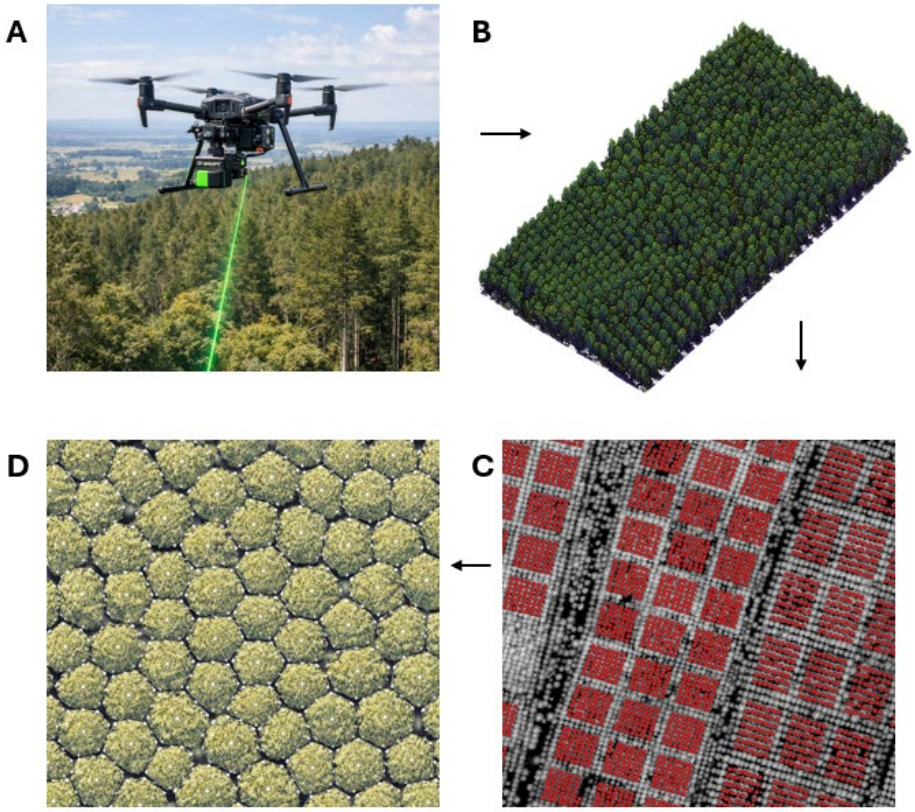



**Figure 3.** Overview of UAV-based LiDAR data acquisition and processing workflow. (**A**) UAV-mounted LiDAR system acquiring high-density point cloud data over the forest canopy. (**B**) Representative pre-cyclone UAV LiDAR point cloud coloured by height (Z). (**C**) Pre-cyclone canopy height model (CHM) with detected individual tree tops indicated by red points. (**D**) Individual tree crown delineation derived from the pre-cyclone CHM using a marker-controlled watershed segmentation approach.

Additional LiDAR data were used to compute a digital terrain model (DTM) and CHM for an area of approximately 63,000 hectares, which was needed to account for the influence of the broader landscape on the local wind climate. The data used to calculate these layers came from the Waikato Regional Council aerial LiDAR acquisition carried out in 2021, which were accessed through Land Information New Zealand (LINZ). These data were collected with a nominal mean point density of 10 points/m$^2$, with up to 5 returns recorded.

### *2.4. Data Preparation and Derived Variables*

In combination, the field and remote sensing datasets provided detailed records for every tree in the trial. These included measurements of DBH (pre-cyclone field sampling), tree height, crown volume and width (pre-cyclone LiDAR acquisition), spatial position, and damage status recorded after the cyclone (pre- and post field sampling).

The tree slenderness coefficient (TSC) was calculated as height (m) divided by DBH (cm). Tree volume was determined from basal area and height using the following equation [27]:

$$V = h \times ba \times (a \times (h - 1.4)^{-b} + c) \quad (1)$$

where $h$ is the tree height, $ba$ is the basal area, and parameters $a$, $b$, and $c$ have values of, respectively, 0.860, 0.972, and 0.340. This function was developed using an extensive dataset from radiata pine stands located in the same region as the study site [27]. As described above, the LiDAR variable zmax was used for tree height. Tree volume was determined for

individual trees prior to the cyclone. Following the cyclone, total stem volume, expressed on a per hectare basis, was determined for all treatment × genotype × block combinations as the product of the pre-cyclone mean tree volume and the post-cyclone stocking.

A summary of all mean pre-cyclone structural attributes, by treatment, is shown in Table 1. Overall, there was very little consistent treatment variation in height. Tree diameter was higher within the two low stocking treatments, while TSC was higher within the high stocking treatments. Mean stem volume did not show a marked trend between treatments. Both crown width and volume were markedly higher in the low stocking treatments.

**Table 1.** Statistics for structural attributes of trees, by treatment, within the trial, determined prior to the cyclone. Shown are the mean, followed by the standard error, for height, diameter at breast height (DBH), tree slenderness coefficient (TSC), stem volume, crown width, and crown volume. Values shown were determined from plot level data.

| Structural Attribute | High Stocking Cultivation | High Stocking No Cultivation | Low Stocking Cultivation | Low Stocking No Cultivation |
|---|---|---|---|---|
| Height (m) | 9.88 (0.176) | 10.42 (0.187) | 9.91 (0.157) | 9.87 (0.160) |
| DBH (cm) | 14.7 (0.246) | 16.1 (0.243) | 16.2 (0.250) | 16.2 (0.263) |
| TSC (m/cm) | 0.690 (0.0056) | 0.662 (0.0053) | 0.629 (0.0051) | 0.624 (0.0053) |
| Stem volume ($m^3$) | 0.0772 (0.0034) | 0.0950 (0.0037) | 0.0922 (0.0035) | 0.0922 (0.0040) |
| Crown width (m) | 3.54 (0.0228) | 3.52 (0.0168) | 4.28 (0.0230) | 4.26 (0.0305) |
| Crown volume ($m^3$) | 36.9 (1.03) | 41.7 (1.09) | 51.3 (1.23) | 53.2 (1.57) |

### 2.5. Statistical Analyses

All statistical analyses were carried out in R [26] using both individual tree records and summaries aggregated by treatment × genotype × block, i.e., plot level (144 plots in total). For descriptive purposes, we plotted the proportions of trees suffering stem breakage, overturning, or total damage by each silvicultural treatment and genotype combination.

Three separate binomial generalized linear mixed models (GLMMs) with a logit link were fitted to model tree-level breakage, overturning, and total damage. Treatment, genotype, and their interaction were specified as fixed effects. Random intercepts were included for block nested within treatment and plot, to, respectively, account for the experimental design and clustering of trees within plots. Where the treatment × genotype interaction was not significant, it was removed and the model was refitted with main effects only.

Relationships between tree structural metrics and damage frequency, for the two damage types, were examined using linear regression at the plot level (treatment × genotype × block; n = 144). For each plot, we calculated the proportion of trees that broke and the proportion that overturned, and plotted these against the mean plot level DBH, height, TSC, crown width, crown volume, and stem volume. Separate simple linear regressions were fitted for each structural metric against the proportion of trees broken and overturned.

### 2.6. Wind Climate Modelling

The local wind environment at the trial site was characterised using two linearised airflow models developed by the Danish Technical University (DTU): WAsP (Wind Atlas Analysis and Application Programme [28]) and WEng (WAsP Engineering [29]). WAsP was used to model the terrain- and land-use-corrected 20-year mean wind climatology [30], while WEng was used to simulate the extreme wind field associated with Cyclone Gabrielle [31].

Wind data were obtained from the Turangi meteorological station (−38.97352°, 175.7908°), located approximately 13 km north of the trial site, comprising 10-min mean wind speeds for WAsP and 10-min gust wind speeds for WEng. Both models required a combined topography and surface roughness map of the surrounding landscape. A DTM

was resampled from 1 m to 10 m resolution and processed using the DTU WAsP QGIS plugin.

Surface roughness was derived from the New Zealand Land Cover Database (LCDB [32]) by matching land-cover classes to equivalent CORINE Land Cover types with recommended roughness-length values [33,34]. The resulting elevation–roughness map allowed terrain and land-cover effects on wind flow to be accounted for when translating the Turangi wind record to the study site. In combination, the WAsP-derived mean climatology and WEng-derived cyclone wind field provide spatially explicit representations of local wind hazard under both typical conditions and the specific case of Cyclone Gabrielle.

## 3. Results

### 3.1. Wind Data Analysis

At the study site, the local wind climate is dominated by southerly winds. During the 20-year climatology, winds occur most frequently from SSE, S, N, and NNE, with relatively few events from easterly sectors (Figures 4A and A1). The Weibull distribution in Figure A1 indicates predominantly low to moderate wind speeds, with a mean wind speed of 2.53 m/s, and only a small proportion of stronger winds, peaking at 12 m/s. This pattern suggests that the topography and local exposure funnel the airflow into a largely north–south pattern on this site, with winds oscillating between the two directions.

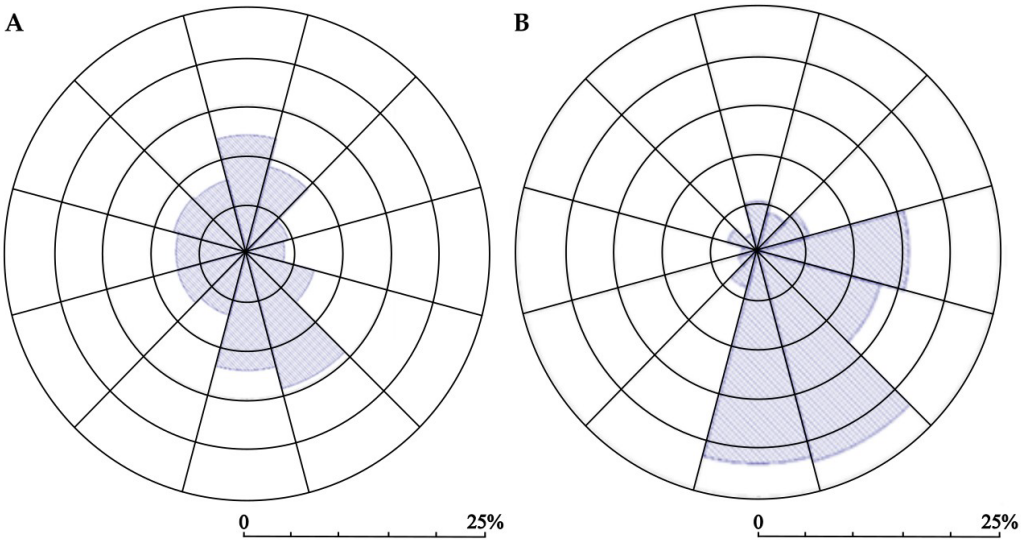



**Figure 4.** Wind roses for the study site showing the frequency of wind directions and speeds for (**A**) the 20-year mean wind climate and (**B**) for winds during Cyclone Gabrielle over a 48-h period.

During the cyclone (Figures 4B and A1B), the directional pattern became even more strongly concentrated toward the south and south–southeast, with some additional moderate winds originating from the east. Over the course of the cyclone, the Weibull histogram and fitted curve in Figure A1 reveal a substantially broader wind-speed distribution with a heavier tail, with a mean wind speed of 2.89 m/s and a maximum wind speed of 20 m/s. This shift indicates both a wider spread of wind speeds and a higher frequency of extreme winds relative to the long-term record.

### 3.2. Overall Damage Patterns

Tree failure across the trial was classified into two distinct modes: breakage and overturning. In total, 16.7% of trees were wind damaged, comprising 10.2% breakage and 6.5% overturning. Figure 5 shows the spatial distribution of observed cyclone damage

across the trial. Breakage and overturning events were dispersed throughout the site, but the low-stocking blocks, particularly those without cultivation, show visibly higher densities of failed trees, whereas areas established at high stocking exhibit more scattered and generally lower damage incidence. Within this overall pattern, breakage is concentrated in the two eastern cultivated areas, while overturning occurs more frequently on the western uncultivated side of the trial. Consistent with the wind climatology, these eastern breakage clusters lie approximately downwind from the dominant SSE winds recorded during the cyclone (Figure 5).

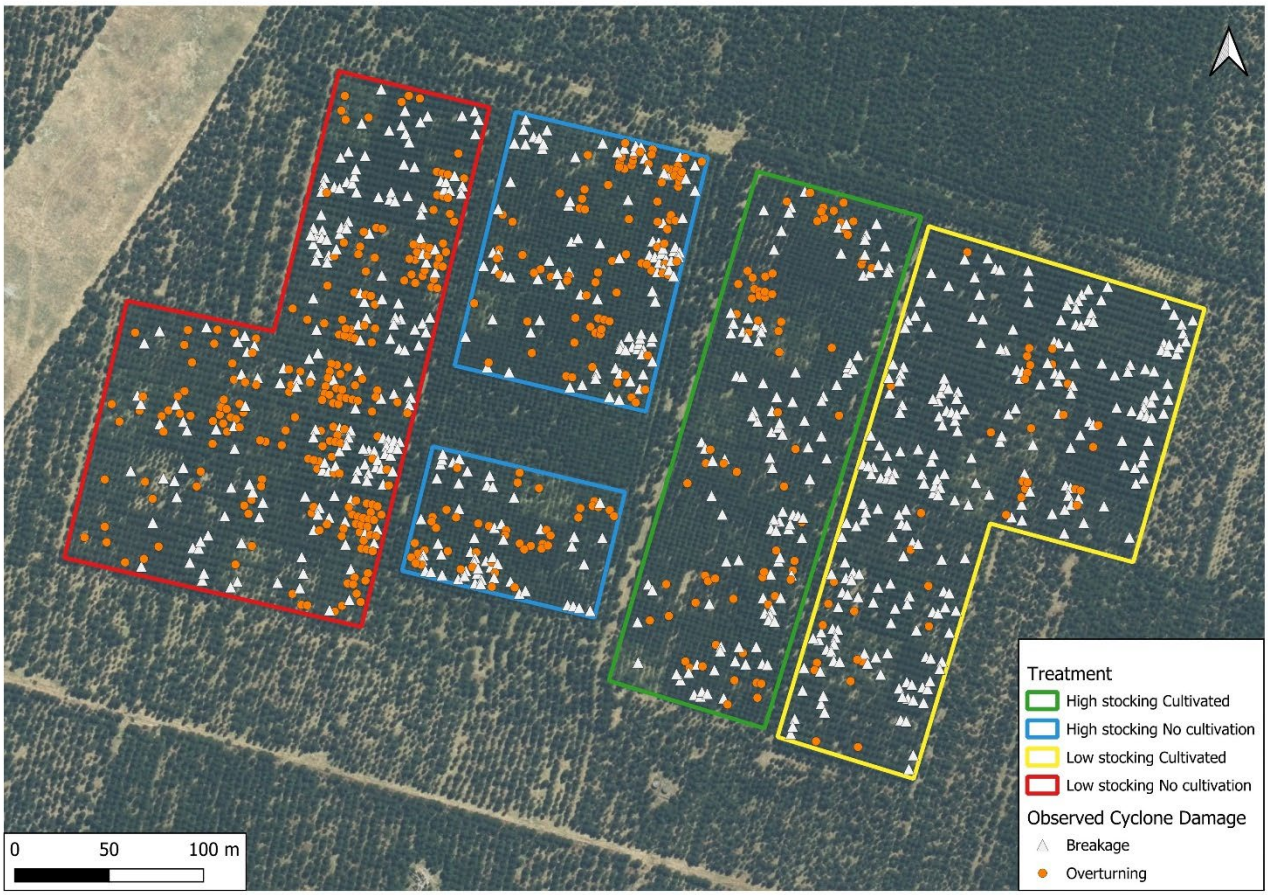



**Figure 5.** Experimental trial layout showing silvicultural treatment blocks and the spatial distribution of cyclone damage (breakage and overturning).

### *3.3. Influence of Treatment and Genotype*

The proportion of trees failing by each mode markedly differed between treatments and genotypes (Table 2). When averaged to the plot level breakage ranged from 0% to 44.9%, while overturning ranged from 0% to 49.0%. The highest values for both failure modes were recorded in the uncultivated low stocking treatment (Appendix A Table A1).

**Table 2.** Percentage (%) of trees damaged by breakage, overturning, or total damage (any failure) across silvicultural treatments (top) and genotypes (middle). The analysis of variance (bottom) shows the Chi-square, followed by *p*-value categories from three separate binomial GLMMs modelling stem breakage, overturning, and total damage as functions of silvicultural treatment, genotype, and their interaction. Asterisks *** and **, respectively, represent significance at $p = 0.001$ and 0.01; ns represents not significant at $p = 0.05$.

| Treatment | Breakage (%) | Overturning (%) | Total Damage (%) |
|---|---|---|---|
| High stocking Cultivated | 6.4 | 4.0 | 10.4 |
| High stocking No cultivation | 8.7 | 7.4 | 16.1 |
| Low stocking Cultivated | 14.5 | 2.2 | 16.7 |
| Low stocking No cultivation | 11.2 | 12.3 | 23.5 |
| Genotype | Breakage (%) | Overturning (%) | Total Damage (%) |
| 1 (*Pinus radiata* × *attenuata* hybrid) | 3.9 | 3.6 | 7.5 |
| 2 | 11.6 | 10.9 | 22.5 |
| 3 | 8.2 | 15.0 | 23.2 |
| 4 | 10.3 | 7.2 | 17.5 |
| 5 | 25.4 | 4.1 | 29.5 |
| 6 | 7.1 | 5.9 | 13.0 |
| 7 | 10.8 | 4.6 | 15.4 |
| 8 | 5.2 | 1.4 | 6.6 |
| 9 | 3.3 | 4.0 | 7.3 |
| 10 | 18.2 | 3.9 | 22.1 |
| 11 | 8.5 | 6.9 | 15.4 |
| 12 (GF19 seedlot) | 9.8 | 10.3 | 20.1 |
| Analysis of variance | Breakage | Overturning | Total damage |
| Treatment | 22.0 *** | 54.5 *** | 25.7 *** |
| Genotype | 219.6 *** | 43.8 *** | 133.4 *** |
| G × T | 64.1 *** | ns | 61.7 ** |

#### 3.3.1. Breakage

Stocking and cultivation both exerted strong and highly significant effects on stem breakage ($\chi^2 = 22.0$, $p < 0.001$), although the magnitude and direction of these effects differed (Table 2). Breakage was consistently higher in the low stocking (mean = 12.9%) than in the high stocking treatments (mean = 7.6%). The impacts of cultivation on breakage were more complex and interactive: cultivation reduced breakage under high stocking (6.4 vs. 8.7%) but increased breakage under low stocking (14.5 vs. 11.2%).

Genotype also had a very strong effect on breakage ($\chi^2 = 219.6$, $p < 0.001$). Damage ranged from only 3.3% to 5.2% in clones 8, 9 and 3.9% in the *P. radiata* × *attenuata* cross (genotype 1) to 25.4% in the most susceptible genotype 5 (Table 2). This eight-fold variation among genotypes highlights substantial genetic differences in susceptibility to stem failure under extreme wind loading. The GF19 seedlot had a breakage of 9.8%, which was similar to the mean value of 10.9% observed across the 10 radiata pine clones. The significant G × T interaction ($\chi^2 = 64.1$, $p < 0.001$) indicates that the relative ranking of genotypes for breakage differed among treatments as clearly illustrated in Figure 6. Breakage was consistently low across treatments for genotypes 8 and 9 (Figure 6).

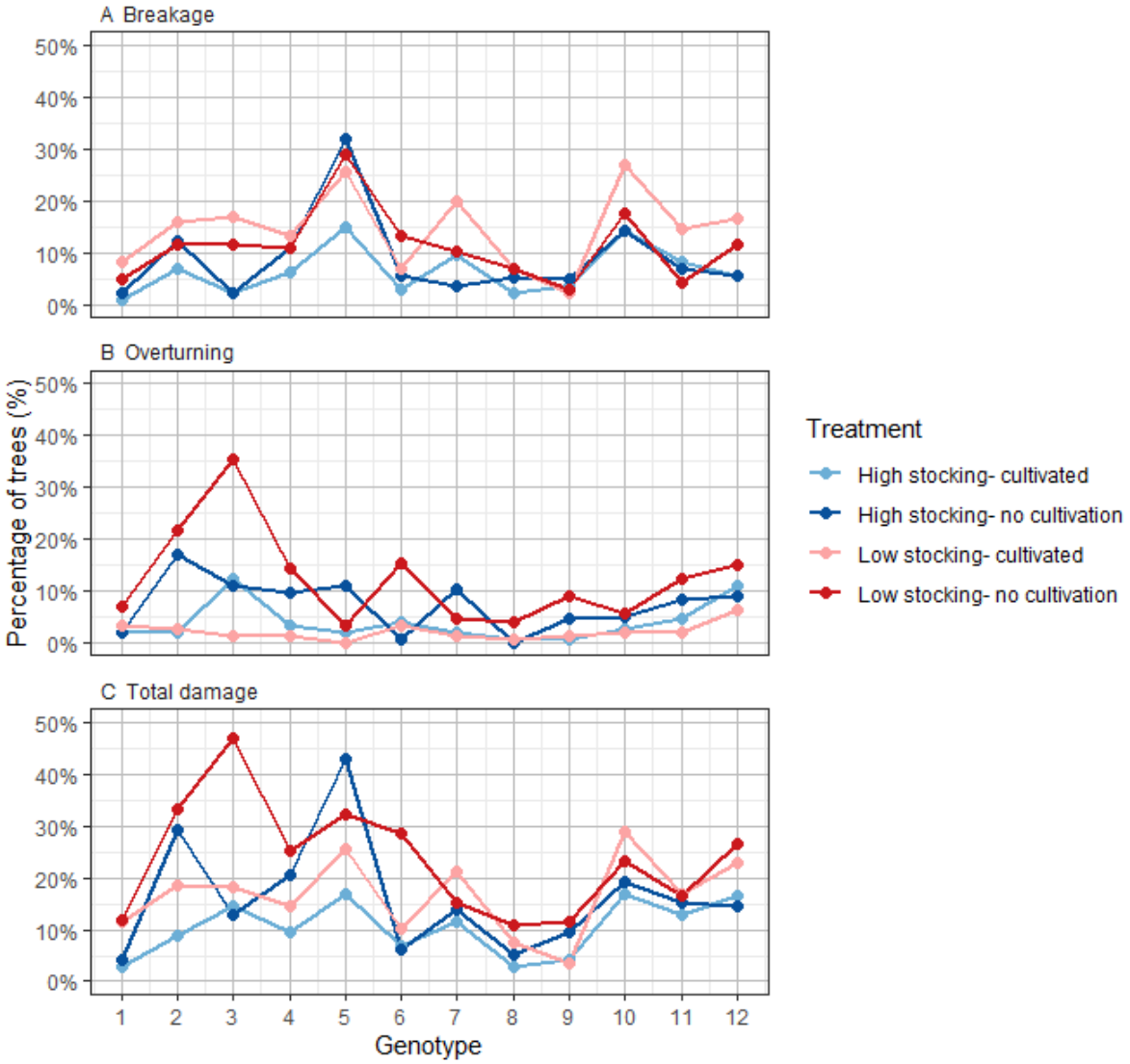



**Figure 6.** Percentage of trees damaged by genotype and silvicultural treatment, showing (**A**) stem breakage, (**B**) overturning, and (**C**) total damage (breakage plus overturning).

### 3.3.2. Overturning

Overturning showed the strongest treatment responses of the three damage components ($\chi^2 = 54.5$, $p < 0.001$), with clear and contrasting effects of stocking and cultivation (Table 2). Damage was markedly lower in the two cultivated treatments (mean = 3.1%) than the uncultivated treatments (mean = 9.9%). The impacts of stocking on overturning interacted with cultivation. While cultivation markedly reduced the incidence of overturning this impact was far more pronounced for the low stocking treatment (2.2 vs. 12.3%) than the high stocking treatment (4.0 vs. 7.4%).

Genotypic effects on overturning were also pronounced ($\chi^2 = 43.8$, $p < 0.001$), with damage ranging from 1.4% for genotype 8 to 15.0% for genotype 3. The *P. radiata* × *attenuata* hybrid (genotype 1) was the second least susceptible genotype to overturning with an observed overturning of 3.6% (Table 2). In contrast, the GF19 seedlot had the third highest overturning rate of 10.3% which markedly exceeded the mean overturning of 6.4% for the 10 radiata pine clones (genotypes 2–11).

The G × T interaction was not significant ($p = 0.27$) demonstrating that treatment impacts on overturning were relatively uniform across genotypes. It was notable that within the low stocking treatment, overturning for all genotypes was lower under cultivation than

the no cultivation treatment (Figure 6). Overturning for genotypes 8, 10 and the *P. radiata* × *attenuata* cross (genotype 1) were consistently low across all treatments (Figure 6).

#### 3.3.3. Total Damage

Patterns in total damage significantly varied between treatments ($\chi^2 = 25.7$, $p < 0.001$). Total damage was higher for areas with low stocking (mean = 20.1%) than high stocking (mean = 13.3%). Uncultivated areas had higher total damage (mean = 19.8%) than cultivated areas (mean = 13.6%) and there was little interaction between the impacts of cultivation and stocking on total damage (Table 2).

Total damage also varied strongly among genotypes ($\chi^2 = 133.4$, $p < 0.001$). Total damage ranged from 6.6% to 7.3% in genotypes 8 and 9, and 7.5% in the *P. radiata* × *attenuata* hybrid (genotype 1) to 29.5% in the most severely damaged genotype 5. This four-fold variation in total damage indicates that genetic control over vulnerability to cyclone damage is more important than the silvicultural setting. Total damage in the GF19 seedlot was 20.1% which exceeded the mean value of 17.3% for the 10 radiata pine clones (genotypes 2–11).

The G × T term for total damage was significant ($\chi^2 = 61.7$, $p < 0.01$) indicating a varied ranking across the four treatment combinations for the 12 genotypes (Figure 6). Total damage was relatively low across all treatments for genotypes 8, 9 and the *P. radiata* × *attenuata* cross (genotype 1).

### *3.4. Relationships Between Tree Metrics and Damage*

Using the 144 plot observations, linear regressions were fitted between mean structural metrics and the percentage of trees damaged (Figures 7 and 8). Breakage significantly increased with larger DBH, greater height (Figure 7), wider crowns, and larger stem and crown volumes (Figure 8). There was a significant negative relationship between TSC and breakage indicating that less slender, more tapered trees were more prone to stem failure.

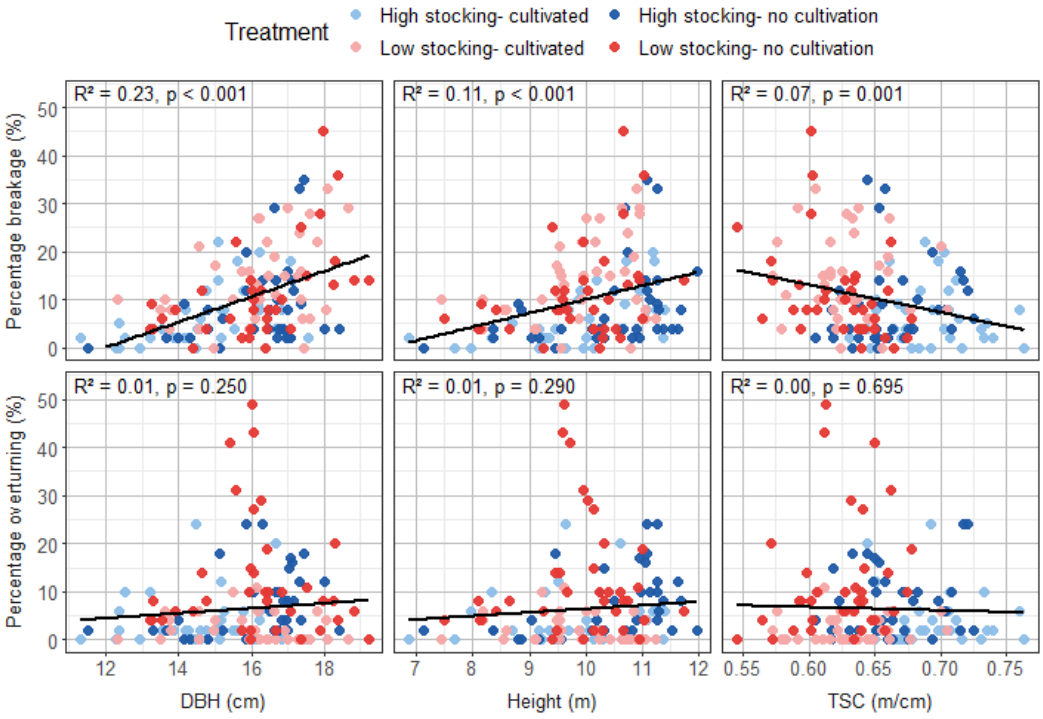



**Figure 7.** Relationships between stand-level structural metrics (diameter at breast height (DBH), tree slenderness coefficient (TSC), and height) and the percentage of trees damaged by stem breakage

(**top row**) or overturning (**bottom row**) by the four treatments. TSC was calculated as height (m) divided by DBH (cm). Linear lines of best fit (solid black lines) are shown and for these relationships the coefficient of determination ($R^2$) and $p$ value are displayed in the top left of each panel.

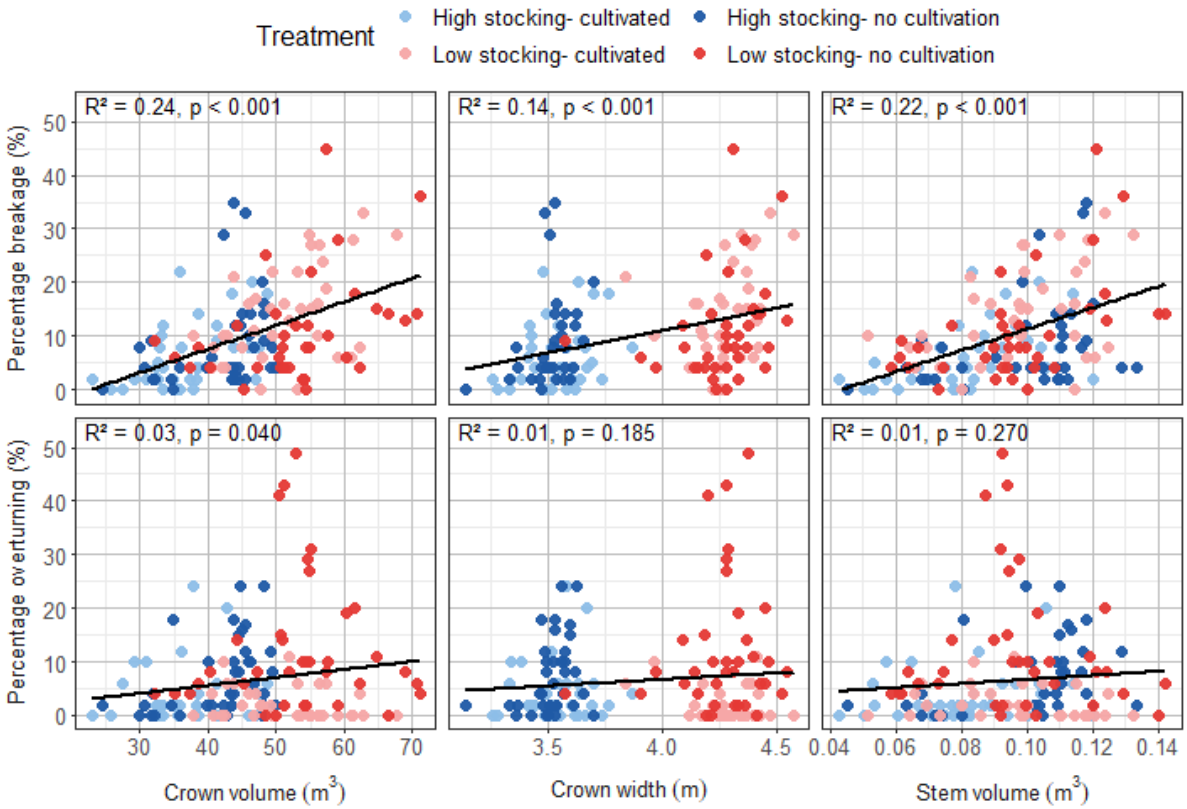



**Figure 8.** Relationships between the stand-level attributes, crown volume, crown width, and stem volume, and the percentage of trees damaged by stem breakage (**top row**) or overturning (**bottom row**). Linear lines of best fit are shown (solid black lines) and for these relationships the coefficient of determination ($R^2$) and $p$ value are displayed in the top left of each panel.

In contrast, overturning was only significantly correlated with one structural attribute. Crown volume exhibited a marginally significant ($p$ = 0.04) positive relationship with overturning (Figure 8). No significant relationships were found between overturning and the remaining tree structural metrics.

### *3.5. Impact of the Cyclone on Tree Volume*

There was a wide range in growth rate between the 12 genotypes (Table A1). For the high stocking treatments, mean tree volume prior to the cyclone ranged widely across the 12 genotypes by two-fold for the high stocking cultivated (0.049–0.115 $m^3$) and no-cultivation treatments (0.059–0.125 $m^3$). Across the low stocking treatments, mean tree volume ranged two-fold for the cultivated (0.062–0.119 $m^3$) and no-cultivation treatments (0.067–0.124 $m^3$). Among the 12 genotypes, mean tree volume was the lowest for the *P. radiata* × *attenuata* cross while it was low to moderate for the GF19 seedlot. Genotype 7 had the highest mean tree volume among all genotypes for all four treatments and mean tree volumes for clones 10, and 4 were also relatively high (Appendix A Table A1).

Total stem volume per hectare (TSV), determined after the cyclone, provided a means of integrating the effects of mean tree size and wind damage on the 12 genotypes to determine genotype productivity and resilience (Table A1). There was a wide range in TSV across the genotypes (Table A1). Averaged to the genotype level (Table A1), these values varied from two-fold for treatments with low stocking and cultivation (45–77 $m^3$/ha), low

stocking and no-cultivation (39–87 $m^3$/ha), high stocking and cultivation (61–129 $m^3$/ha) and high stocking and no cultivation (73–136 $m^3$/ha).

In general, the genotypes with the highest TSV combined a relatively high growth rate with low to moderate susceptibility to the cyclone (Table A1). Across the four treatments, TSV was highest for clones 7 (mean = 107 $m^3$/ha; range 77–136 $m^3$/ha) and 9 (mean = 91 $m^3$/ha; range 70–118 $m^3$/ha). Clone 7 was the most rapidly growing genotype which sustained low- moderate damage by the wind while Clone 9 combined a moderate to high growth rate with very low wind damage (Table A1). The GF19 seedlot had a moderate TSV for all four treatments (mean = 86 $m^3$/ha; range 63–116 $m^3$/ha) as both growth rate and wind damage were moderate. Despite the low wind damage suffered by the *P. radiata* × *attenuata* hybrid, the TSV after the cyclone was very low (mean = 57 $m^3$/ha; range 45–73 $m^3$/ha) as this genotype had a slow growth rate (Table A1). Under a low stocking, uncultivated regime, which is typical practice throughout New Zealand, Genotype 7 had a high TSV of 87 $m^3$/ha, which exceeded the 63 $m^3$/ha of the widely planted GF19 genotype by 38% (Table A1).

## 4. Discussion

This study demonstrated the significant impact of stocking, cultivation and genotype in determining breakage and overturning from severe wind events. Although overall damage from the cyclone was greatest under low stocking, cultivation reduced the incidence of overturning, particularly in the low-stocking regime, indicating that establishment practices can shift both the magnitude and mode of failure. Across the trial, however, genetic variation in wind damage far exceeded differences between treatments, highlighting the strong genetic influence on wind resistance. When realised productivity was expressed as total stem volume, two clones that combined low–moderate damage with strong growth clearly outperformed the widely planted GF19 seedlot. These results demonstrate how productivity can be maximised by selecting genotypes that jointly optimise growth and mechanical stability under storm events. In the sections that follow, we examine reasons for the prevalence of breakage within the trial (Section 4.1), contextualise relationships found between damage and tree attributes (Section 4.2), examine the implications of genotypic rankings for deployment (Section 4.3), and highlight study limitations and areas for further research (Section 4.4).

### *4.1. Relative Impact of the Cyclone on Breakage and Overturning*

In the study, wind damage associated with Cyclone Gabrielle manifested primarily as stem breakage rather than overturning, with clear differences in the incidence of each failure mode across stocking and cultivation treatments. Wind damage occurs when wind loading on parts of the tree exceeds the structural strength of the roots, stem or crown, and can range from minor crown damage through to complete stem failure or uprooting [35]. Both low-stocking treatments had the highest combined incidence of breakage and overturning, indicating that reduced mutual shelter and greater exposure of individual crowns substantially increased effective wind loading at the tree level during Cyclone Gabrielle. In contrast, closer spacing in high-stocking plots likely enhanced mutual support through mechanisms such as crown clashing that dissipates storm energy [36], while lower stand porosity reduced wind penetration and crown-level wind loading. These stocking-related effects are consistent with previous studies in radiata pine and other conifer species [37–39] and with mechanistic wind-risk frameworks and ForestGALES-type semi-mechanistic wind-risk models. These studies show marked reductions in critical wind speeds of damage as stocking declines and trees become more widely spaced and crown-dominated in their interaction with the wind [40,41]

In many mature conifer stands, overturning has been reported as the predominant failure mode, particularly on weaker or wetter soils where anchorage is a limiting factor [11]. Tree-pulling experiments and mechanistic models indicate that stem breakage generally requires higher wind loading than overturning, because the stem must exceed its resistive breaking moment whereas uprooting occurs once root–soil anchorage is overcome [11]. The dominance of breakage observed here is likely attributable to the age and structural state of the trial, in which trees were tall enough to experience substantial bending under cyclone loading while retaining strong root–soil anchorage on well-drained sandy loam soils [11]. Under these conditions, wind loading during Cyclone Gabrielle more often exceeded stem bending strength than root–soil resistance, resulting in a higher incidence of breakage than overturning.

A lower incidence of overturning under cultivation, which was most evident in the low-stocking treatment, suggests that improved rooting conditions strengthened root–soil anchorage. Under extreme wind loading this likely shifted failure away from the root–soil system and towards the stem, contributing to a higher incidence of stem breakage. In contrast, under high stocking the anchorage benefits of cultivation appeared more limited, possibly because greater below-ground competition constrained root system expansion. Tree stability against overturning is strongly influenced by root plate size and geometry, with larger and deeper root systems increasing the resisting moment required for uprooting, as demonstrated in tree-pulling experiments and mechanistic anchorage models [11,42,43]. Root–soil anchorage has been shown to scale with root plate diameter, rooting depth and soil shear strength, all of which contribute to overturning resistance [42,43]. Although root architecture was not directly assessed in this study, cultivation likely enhanced root penetration and lateral spread through reduced soil compaction and improved soil structure, thereby increasing effective root plate development. The stronger cultivation effect under low stocking is consistent with greater opportunity for below-ground expansion when inter-tree competition is reduced.

Trees respond to both mean and extreme winds by reallocating resources to promote stability through responsive root development, morphological adjustments such as increased taper or crown asymmetry, and structural changes in stem mechanical properties (for example, the formation of reaction wood) [44–46]. At the trial site, long-term exposure to predominantly south and south-east winds, with additional loading from northerly sectors, is likely to have influenced tree form and anchorage through directional root reinforcement and asymmetric growth. During Cyclone Gabrielle, winds arrived predominantly from similar sectors. Consequently, loading occurred largely along previously experienced directions, favouring relatively strong root–soil anchorage while simultaneously increasing stem bending stresses and the likelihood of breakage rather than overturning.

### *4.2. Relationships Between Tree Attributes and Damage*

In contrast to expectations based on established relationships between tree form and wind resistance, tree slenderness coefficient (TSC) was not positively associated with wind damage in this study [14–16]. Overturning showed no significant relationship with TSC, while stem breakage exhibited a significant but inverse relationship, with higher breakage occurring in less slender trees. This likely reflects the young developmental stage of the plantation, in which height-driven mechanical instability is less developed. Under these conditions, variation in TSC may instead reflect differences in tree form associated with crown development rather than susceptibility to leverage-related failure. Crown architecture emerged as the dominant structural influence on damage outcomes. Stem breakage increased with DBH and height, consistent with size-related increases in bending stress [47], and was positively associated with crown width and crown volume, reflecting

increased aerodynamic drag generated by larger crowns [48,49]. Breakage also increased with stem volume, which has been linked to greater bending moments acting on the stem during wind events [50]. In contrast, overturning was associated only with crown volume, consistent with increased wind loading on the root–soil system due to greater effective sail area [48,49].

### 4.3. Genotypic Variation in Damage Resistance and Impact on Productivity

The study revealed clear genotypic differences in the balance between overturning and stem breakage, with wide genetic variation in damage for both modes that was only partly explained by the measured structural variables. This suggests that wind resistance is controlled by multiple interacting traits, including stem form, wood properties, crown architecture and rooting, rather than by a single 'wind-firmness' attribute [35]. Genetic variation in susceptibility to windthrow has been demonstrated in other conifers; for example, family-level differences in windthrow have been documented in young Douglas fir, providing direct evidence that genetic background can influence storm damage under comparable stand conditions [51]. To our knowledge, however, no peer reviewed studies have explicitly quantified clone- or genotype-level differences in storm damage incidence and failure mode for radiata pine. Consequently, this trial provides novel evidence that genetic background can influence both overall susceptibility and the dominant failure mode across silvicultural treatments.

The wide variation in genotype susceptibility to wind was an important contributor to post-cyclone total productivity highlighting the importance of tree breeding to mitigate impacts of windthrow [45,51]. Using total stem volume per hectare (TSV) as an integrated measure of resilience and productivity, radiata pine clones 7 and 9 consistently ranked highest across treatments (mean TSV of 107 and 91 $m^3$ $ha^{-1}$, respectively). Clone 7 achieved the greatest TSV as it had a high growth rate and low–moderate cyclone damage, while clone 9 achieved a high TSV through pairing a moderate–high growth rate with very low wind damage (Table A1). Importantly, TSV was higher in four of the ten clones than the GF19 seedlot, highlighting gains that can be made over typically deployed planting material through selection of highly productive, wind resistance clones. Despite very low wind damage, the *P. radiata* × *P. attenuata* hybrid (genotype 1) had the lowest TSV as it was the slowest growing genotype. Our results suggest that selecting for genotypes that jointly optimise growth and mechanical stability offers a direct pathway to maximise post-storm productivity.

### 4.4. Limitations and Further Research

A key limitation of this study was that post-cyclone TSV was estimated as the product of the pre-cyclone mean tree volume, and the post-cyclone stocking of undamaged trees. This approach assumes that relative size rankings among genotypes and treatments did not change materially during the approximately six-month interval between the pre-cyclone measurements (August 2022) and Cyclone Gabrielle (February 2023). As trees would have continued to grow over this six-month interval, the estimated TSV values are likely to slightly underestimate true TSV immediately prior to the cyclone. However, as six months is a relatively low proportion of the tree age (seven years), this approach is unlikely to greatly affect relative rankings between genotypes and the reported outcomes. The analyses also assume that there was little additional damage between the cyclone and the post-cyclone measurements, which were made 19 months later. This does seem to be a reasonable assumption as there were no significant wind events over this period.

With projections indicating potential changes in the frequency, intensity and tracks of severe storms affecting New Zealand, reliable prediction of wind damage is becoming

increasingly important for forest management and investment decisions [1,52]. The treatments, genotypes and structural predictors highlighted in this study are likely to vary in their importance among sites, storm events and tree species. This emphasises the need for further event-based studies across a wider range of environments and tree species and a framework for integrating these data so that predictions can be generalised. The relationships and treatment effects reported here were observed under a specific combination of soil type, rainfall conditions, stand age and storm characteristics, and their strength and direction may differ under alternative soil conditions, hydrological regimes, developmental stages or wind climates. Longer-term consequences of storm damage were also beyond the scope of this study. Continued monitoring would be required to determine whether initial differences in damage translate into sustained differences in growth allocation, stem form or wood properties.

A logical next step would be to test the applicability of a hybrid-mechanistic wind-risk model such as ForestGALES [40] to this trial. Model validation should be undertaken by comparing model-predicted critical wind speeds for overturning and breakage against observed damage patterns from Cyclone Gabrielle. Such mechanistic models explicitly integrate tree geometry, soil anchorage and wind loading processes, and are therefore better suited to resolving causal relationships than observational regression analyses alone [53]. Analyses and simulations based on a fitted model would enable forest managers to optimise stocking, clone selection and rotation length to minimise risk while maintaining productivity [41]. Validation across multiple sites that comprise contrasting soil types, stand ages and wind climates would allow testing of whether the treatment and genotypic patterns observed here persist under different environmental constraints.

## 5. Conclusions

Substantial variation in cyclone impacts were observed across both stand treatments and genotypes, highlighting that wind damage in young radiata pine is strongly contingent on the interaction between stand structure, tree form, wood properties, rooting and exposure. Total damage was highest under low stocking, consistent with reduced mutual shelter and larger crowns, whereas high-stocking plots generally experienced lower damage. Importantly, these patterns translated into clear differences in realised productivity, with TSV capturing the combined effects of growth and storm losses. Genotypes that paired strong growth with low–moderate damage had the highest TSV and these values of TSV greatly exceeded that of the unselected GF19 seedlot, which has been widely planted throughout New Zealand.

Genotypic differences in both damage susceptibility and post-storm TSV indicate that genetic background can materially influence stand-level outcomes under extreme wind events. These results reinforce the value of selecting genotypes and prescribing establishment regimes that jointly optimise growth and stability, rather than maximising growth alone. This approach will become increasingly important as severe storms are expected to increase. Finally, incorporating these detailed, tree-level damage observations into a ForestGALES validation and calibration framework would strengthen wind-risk predictions and better support decisions around stocking, genotype choice, and rotation planning for New Zealand plantations.

**Author Contributions:** Conceptualization, M.S.W., K.H. and T.L.; methodology, M.S.W., K.H. and T.L.; software, K.H. and S.J.; validation, K.H.; formal analysis, M.S.W., K.H. and T.L.; investigation, K.H., M.S.W. and T.L.; resources, M.S.W. and T.L.; data curation, M.S.W., N.C. and S.J.; writing—original draft preparation, K.H., M.S.W. and T.L.; writing—review and editing, K.H., M.S.W., T.L., N.C., S.J. and J.C.S.; visualization, K.H. and M.S.W.; supervision, M.S.W. and T.L.; project administration,

M.S.W. and N.C.; funding acquisition, M.S.W. All authors have read and agreed to the published version of the manuscript.

**Funding:** We thank Forest Growers Research for funding this study (CN013708-FGR407). We are also grateful to the Catalyst Fund—Seeding (CSG-FRI2401) for funding exchanges between Scion Group and Forest Research (Scotland). Funding for the ground-based tree measurements was provided by the Resilient Forest program through the Forest Growers Levy Trust, with support from the NZ Forest Owners Association (FOA) and the NZ Farm Forestry Association (FFA) (C04X1703). We thank Lake Taupo Forest Trust for allowing us access to the trial data. Pre-cyclone LiDAR data collection and processing was funded by Ministry of Business, Innovation, and Employment (MBIE) through the programme entitled "Seeing the forest for the trees: transforming tree phenotyping for future forests" (programme grant number: C04X2101).

**Data Availability Statement:** The datasets presented in this article are not available because of privacy restrictions.

**Acknowledgments:** We thank Lake Taupō Forest Management and NZ Forest Managers for granting access to the trial site. The authors also thank Scion technical staff who contributed to fieldwork and LiDAR data collection. We further acknowledge Scion's Accelerator Trial team for providing various datasets used in this study.

**Conflicts of Interest:** The authors declare no conflicts of interest.

## Abbreviations

The following abbreviations are used in this manuscript:

| | |
|---|---|
| CHM | Canopy Height Model |
| DBH | Diameter at breast height |
| DTM | Digital Terrain Model |
| LiDAR | Light Detection and Ranging |
| RGB | Red, Green, Blue |
| TSC | Tree slenderness coefficient |
| TSV | Total stem volume |
| UAV | Unmanned aerial vehicle |
| WAsP | Wind Atlas Analysis and Application Programme |

## Appendix A

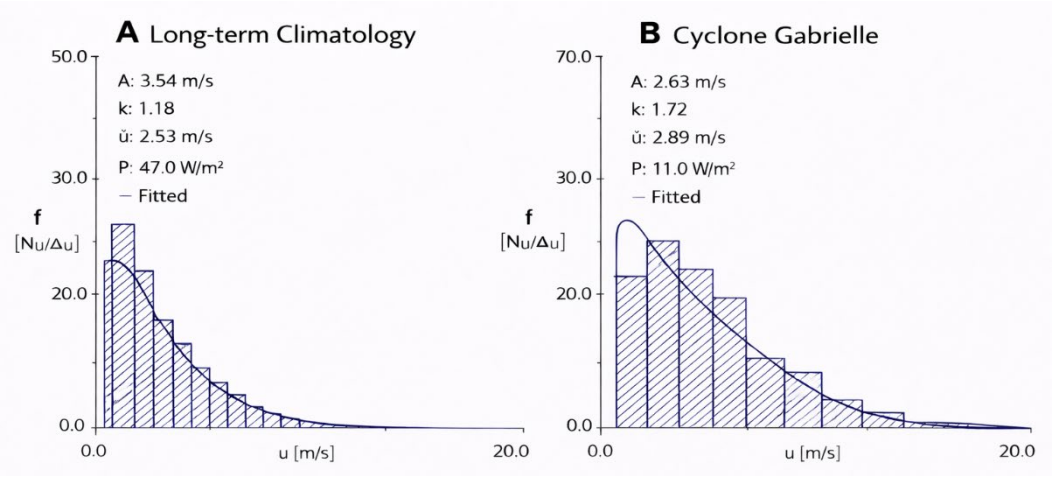



**Figure A1.** Weibull distributions of wind speed at the study site showing frequency density (f, $N_u/\Delta u$) as a function of wind speed (ŭ, m/s). Bars represent observed wind-speed frequencies and

solid lines show fitted Weibull probability density functions. Reported parameters include the Weibull scale parameter (A, m/s), shape parameter (k), mean wind speed (ŭ, m/s), and mean wind power density (P, W/m$^2$). Panel (**A**) shows the long-term (20-year) wind climatology for all wind directions at the study site, and panel (**B**) shows the wind-speed distribution during Cyclone Gabrielle.

**Table A1.** Summary of wind damage incidence and tree structural attributes across genotype × treatment groups. Shown is the stocking post-cyclone, the percentage breakage, overturning and total damage. Dimensions include mean diameter at breast height (DBH), height and volume determined pre-cyclone. The post-cyclone total stem volume is determined as the product of the pre-cyclone mean tree volume and post-cyclone stocking. Also shown are the tree LiDAR derived metrics, mean crown width, crown volume and the tree slenderness coefficient (TSC), which were extracted pre-cyclone. For the percent total damage the shading, within each treatment, represents low (green), moderate (orange) and high (red) damage. For the mean and total stem volume the shading represents low (red), medium (orange) and high (red) values. Abbreviations for the treatments are as follows: high stocking (HS); low stocking (LS); cultivated (cult.); no cultivation (no cult.).

| Treatment | Genotype | Stocking Post-Cyclone | % Breakage | % Over-turning | % Total Damage | Mean DBH | Mean Height | Mean Tree Volume | Total Stem Volume | Mean Crown Width | Mean Crown Volume | Mean TSC |
|---|---|---|---|---|---|---|---|---|---|---|---|---|
| | | Stems/ha | % | % | % | cm | m | m$^3$ | m$^3$/ha | m | m$^3$ | m/cm |
| HS-cult. | 1 | 1247 | 0.7 | 2 | 2.7 | 12.0 | 7.5 | 0.049 | 61 | 3.29 | 25.4 | 0.65 |
| HS-cult. | 2 | 1169 | 6.8 | 2 | 8.8 | 14.7 | 10.1 | 0.082 | 96 | 3.47 | 36.5 | 0.71 |
| HS-cult. | 3 | 1090 | 2.1 | 12.3 | 14.4 | 13.5 | 9.1 | 0.067 | 73 | 3.46 | 33.1 | 0.70 |
| HS-cult. | 4 | 1160 | 6.1 | 3.4 | 9.5 | 15.2 | 10.3 | 0.087 | 101 | 3.65 | 39.3 | 0.69 |
| HS-cult. | 5 | 1064 | 15 | 2 | 17.0 | 15.1 | 10.0 | 0.083 | 88 | 3.44 | 34.1 | 0.67 |
| HS-cult. | 6 | 1169 | 2.8 | 4.2 | 6.9 | 14.0 | 9.6 | 0.072 | 85 | 3.50 | 34.1 | 0.71 |
| HS-cult. | 7 | 1125 | 9.6 | 2.1 | 11.6 | 17.2 | 11.3 | 0.115 | 129 | 3.70 | 47.2 | 0.66 |
| HS-cult. | 8 | 1195 | 2.1 | 0.7 | 2.8 | 13.1 | 9.0 | 0.062 | 74 | 3.61 | 32.9 | 0.72 |
| HS-cult. | 9 | 1186 | 3.5 | 0.7 | 4.2 | 15.1 | 10.1 | 0.084 | 100 | 3.56 | 37.2 | 0.68 |
| HS-cult. | 10 | 1020 | 14.2 | 2.8 | 17.0 | 15.5 | 10.7 | 0.093 | 95 | 3.65 | 42.8 | 0.71 |
| HS-cult. | 11 | 1108 | 8.2 | 4.8 | 13.0 | 15.5 | 10.9 | 0.092 | 102 | 3.58 | 41.1 | 0.71 |
| HS-cult. | 12 | 1064 | 5.5 | 11 | 16.4 | 16.0 | 10.1 | 0.095 | 101 | 3.57 | 39.1 | 0.64 |
| HS-no cult | 1 | 1221 | 2.1 | 2.1 | 4.1 | 12.8 | 7.9 | 0.059 | 73 | 3.28 | 29.9 | 0.65 |
| HS-no cult | 2 | 907 | 12.2 | 17 | 29.3 | 16.6 | 11.1 | 0.108 | 98 | 3.55 | 45.2 | 0.69 |
| HS-no cult | 3 | 1108 | 2.1 | 11 | 13.0 | 15.0 | 9.6 | 0.082 | 91 | 3.49 | 35.6 | 0.65 |
| HS-no cult | 4 | 1012 | 11 | 9.6 | 20.5 | 16.7 | 11.4 | 0.113 | 114 | 3.57 | 46.6 | 0.70 |
| HS-no cult | 5 | 733 | 32 | 10.9 | 42.9 | 17.1 | 11.0 | 0.113 | 83 | 3.51 | 43.8 | 0.65 |
| HS-no cult | 6 | 1169 | 5.6 | 0.7 | 6.3 | 16.0 | 9.9 | 0.094 | 109 | 3.45 | 37.4 | 0.63 |
| HS-no cult | 7 | 1090 | 3.4 | 10.3 | 13.8 | 17.8 | 11.4 | 0.125 | 136 | 3.59 | 48.2 | 0.64 |
| HS-no cult | 8 | 1151 | 5 | 0 | 5.0 | 14.4 | 9.2 | 0.073 | 84 | 3.49 | 33.2 | 0.66 |
| HS-no cult | 9 | 1142 | 4.8 | 4.8 | 9.7 | 16.3 | 10.9 | 0.103 | 118 | 3.48 | 42.7 | 0.69 |
| HS-no cult | 10 | 985 | 14.3 | 5 | 19.3 | 16.6 | 11.0 | 0.108 | 107 | 3.64 | 47.4 | 0.67 |
| HS-no cult | 11 | 1081 | 6.8 | 8.2 | 15.1 | 16.5 | 11.4 | 0.109 | 118 | 3.53 | 46.6 | 0.70 |
| HS-no cult | 12 | 1064 | 5.6 | 9.1 | 14.7 | 17.0 | 10.3 | 0.109 | 116 | 3.60 | 44.1 | 0.62 |
| LS-cult. | 1 | 737 | 8.2 | 3.4 | 11.6 | 13.2 | 7.9 | 0.062 | 45 | 4.20 | 40.4 | 0.63 |
| LS-cult. | 2 | 669 | 15.9 | 2.8 | 18.6 | 16.0 | 10.2 | 0.098 | 66 | 4.08 | 50.3 | 0.66 |
| LS-cult. | 3 | 680 | 17 | 1.4 | 18.4 | 16.4 | 10.1 | 0.102 | 69 | 4.24 | 50.8 | 0.63 |
| LS-cult. | 4 | 703 | 13.1 | 1.4 | 14.5 | 16.6 | 10.4 | 0.105 | 74 | 4.29 | 54.1 | 0.64 |

**Table A1.** *Cont.*

| Treatment | Genotype | Stocking Post-Cyclone | % Breakage | % Over-turning | % Total Damage | Mean DBH | Mean Height | Mean Tree Volume | Total Stem Volume | Mean Crown Width | Mean Crown Volume | Mean TSC |
|---|---|---|---|---|---|---|---|---|---|---|---|---|
| | | Stems/ha | % | % | % | cm | m | $m^3$ | $m^3$/ha | m | $m^3$ | m/cm |
| LS-cult. | 5 | 612 | 25.5 | 0 | 25.5 | 17.2 | 10.5 | 0.111 | 68 | 4.42 | 57.1 | 0.62 |
| LS-cult. | 6 | 737 | 6.9 | 3.4 | 10.3 | 16.3 | 9.9 | 0.097 | 71 | 4.16 | 48.4 | 0.61 |
| LS-cult. | 7 | 646 | 20 | 1.4 | 21.4 | 17.7 | 10.6 | 0.119 | 77 | 4.43 | 59.7 | 0.61 |
| LS-cult. | 8 | 765 | 6.8 | 0.7 | 7.5 | 14.0 | 8.8 | 0.069 | 53 | 4.24 | 42.7 | 0.68 |
| LS-cult. | 9 | 788 | 2.1 | 1.4 | 3.5 | 16.2 | 10.1 | 0.096 | 76 | 4.25 | 49.6 | 0.63 |
| LS-cult. | 10 | 584 | 26.9 | 2.1 | 29.0 | 16.7 | 10.4 | 0.105 | 61 | 4.36 | 57.6 | 0.64 |
| LS-cult. | 11 | 674 | 14.7 | 2.1 | 16.8 | 16.9 | 10.3 | 0.104 | 70 | 4.31 | 53.1 | 0.62 |
| LS-cult. | 12 | 629 | 16.7 | 6.3 | 22.9 | 17.0 | 9.8 | 0.104 | 65 | 4.37 | 51.4 | 0.59 |
| LS-no cult. | 1 | 725 | 4.8 | 6.9 | 11.7 | 13.9 | 8.1 | 0.067 | 48 | 4.05 | 40.9 | 0.60 |
| LS-no cult. | 2 | 555 | 11.6 | 21.8 | 33.3 | 15.4 | 9.7 | 0.088 | 49 | 4.27 | 51.6 | 0.65 |
| LS-no cult. | 3 | 442 | 11.6 | 35.4 | 46.9 | 15.6 | 9.6 | 0.088 | 39 | 4.25 | 49.5 | 0.63 |
| LS-no cult. | 4 | 623 | 10.9 | 14.3 | 25.2 | 17.2 | 10.8 | 0.115 | 71 | 4.35 | 61.0 | 0.63 |
| LS-no cult. | 5 | 555 | 29 | 3.4 | 32.4 | 17.3 | 10.4 | 0.111 | 62 | 4.29 | 55.5 | 0.61 |
| LS-no cult. | 6 | 584 | 13.2 | 15.3 | 28.5 | 15.3 | 9.1 | 0.084 | 49 | 3.99 | 43.6 | 0.61 |
| LS-no cult. | 7 | 703 | 10.3 | 4.8 | 15.1 | 18.2 | 10.7 | 0.124 | 87 | 4.47 | 65.9 | 0.60 |
| LS-no cult. | 8 | 737 | 6.8 | 4.1 | 11.0 | 14.6 | 8.7 | 0.075 | 55 | 4.19 | 43.4 | 0.62 |
| LS-no cult. | 9 | 731 | 2.7 | 8.9 | 11.6 | 16.1 | 10.2 | 0.095 | 70 | 4.23 | 52.1 | 0.64 |
| LS-no cult. | 10 | 618 | 17.6 | 5.6 | 23.2 | 17.2 | 10.7 | 0.113 | 70 | 4.42 | 63.3 | 0.63 |
| LS-no cult. | 11 | 691 | 4.1 | 12.3 | 16.4 | 16.3 | 10.6 | 0.100 | 69 | 4.23 | 55.4 | 0.66 |
| LS-no cult. | 12 | 612 | 11.6 | 15 | 26.5 | 16.9 | 9.8 | 0.104 | 63 | 4.43 | 55.7 | 0.59 |

## References


1. Tamura, Y.; Cao, S. International Group for Wind-Related Disaster Risk Reduction (IG-WRDRR). *J. Wind Eng. Ind. Aerodyn.* **2012**, *104–106*, 3–11. [CrossRef]
2. Watt, M.S.; Holdaway, A.; Camarretta, N.; Locatelli, T.; Jayathunga, S.; Watt, P.; Tao, K.; Suárez, J.C. Mapping windthrow risk in *Pinus radiata* plantations using multi-temporal LiDAR and machine learning: A case study of Cyclone Gabrielle, New Zealand. *Remote Sens.* **2025**, *17*, 1777. [CrossRef]
3. Massey, C.; Leith, K.; Robinson, T.R.; Lukovic, B.; McColl, S.; Carey-Smith, T.; Rosser, B.; Wotherspoon, L.; Smith, H.; Betts, H.; et al. What controlled the occurrence of more than 116,000 human-mapped landslides triggered by Cyclone Gabrielle, New Zealand? *Landslides* **2025**, *22*, 3953–3972. [CrossRef]
4. Harrington, L.J.; Dean, S.M.; Awatere, S.; Rosier, S.; Queen, L.; Gibson, P.B.; Barnes, C.; Zachariah, M.; Philip, S.; Kew, S. *The Role of Climate Change in Extreme Rainfall Associated with Cyclone Gabrielle over Aotearoa New Zealand's East Coast*; Imperial College London: London, UK, 2023.
5. Stone, D.A.; Noble, C.J.; Bodeker, G.E.; Dean, S.M.; Harrington, L.J.; Rosier, S.M.; Rye, G.D.; Tradowsky, J.S. Cyclone Gabrielle as a design storm for northeastern Aotearoa New Zealand under anthropogenic warming. *Earth's Future* **2024**, *12*, e2024EF004772. [CrossRef]
6. New Zealand Forest Owners Association (NZFOA). Facts and Figures 2023/2024: New Zealand Plantation Forest Industry. Available online: https://www.nzfoa.org.nz/resources/publications/facts-and-figures (accessed on 12 December 2025).
7. Moore, J.S.; Tombleson, J.D.; Turner, J.J.; Van, M. Wind effects on juvenile trees: A review with special reference to toppling of radiata pine growing in New Zealand. *Forestry* **2008**, *81*, 377–387. [CrossRef]
8. Watt, M.S.; Kirschbaum, M.U.; Moore, J.R.; Pearce, H.G.; Bulman, L.S.; Brockerhoff, E.G.; Melia, N. Assessment of multiple climate change effects on plantation forests in New Zealand. *For. Int. J. For. Res.* **2019**, *92*, 1–15. [CrossRef]
9. Martin, T.J.; Ogden, J. Wind damage and response in New Zealand forests: A review. *N. Z. J. Ecol.* **2006**, *30*, 295–310.

10. Gardiner, B.; Schuck, A.; Schelhaas, M.-J.; Orazio, C.; Blennow, K.; Nicoll, B. (Eds.) Living with Storm Damage to Forests: What Science Can Tell Us. In *Living with Storm Damage to Forests: What Science Can Tell Us*; European Forest Institute: Joensuu, Finland, 2013.
11. Gardiner, B. Wind damage to forests and trees: A review with an emphasis on planted and managed forests. *J. For. Res.* **2021**, *26*, 248–266. [CrossRef]
12. Locatelli, T.; Tarantola, S.; Gardiner, B.; Patenaude, G. Variance-based sensitivity analysis of a wind risk model: Model behaviour and lessons for forest modelling. *Environ. Model. Softw.* **2017**, *87*, 84–109. [CrossRef]
13. Peltola, H.; Kellomäki, S.; Väisänen, H.; Ikonen, V.-P. A mechanistic model for assessing the risk of wind and snow damage to single trees and stands of Scots pine, Norway spruce, and birch. *Can. J. For. Res.* **1999**, *29*, 647–661. [CrossRef]
14. Hale, S.E.; Gardiner, B.A.; Wellpott, A.; Nicoll, B.C.; Achim, A. Wind loading of trees: Influence of tree size and competition. *Eur. J. For. Res.* **2012**, *131*, 203–217. [CrossRef]
15. Đodan, M.; Perić, S. Windthrow resistance of Norway spruce (*Picea abies* (L.) Karst.) forest cultures—Preliminary results. *S.-E. Eur. For.* **2019**, *10*, 77–88. [CrossRef]
16. Watt, M.S.; Moore, J.R. Modeling spatial variation in radiata pine slenderness (height/diameter ratio) and vulnerability to wind damage under current and future climate in New Zealand. *Front. For. Glob. Change* **2023**, *6*, 1188094. [CrossRef]
17. Merz, B.; Kuhlicke, C.; Kunz, M.; Pittore, M.; Babeyko, A.; Bresch, D.N.; Domeisen, D.I.V.; Feser, F.; Koszalka, I.; Kreibich, H.; et al. Impact forecasting to support emergency management of natural hazards. *Rev. Geophys.* **2020**, *58*, e2020RG000704. [CrossRef]
18. Burdon, R.D.; Li, Y.; Suontama, M.; Dungey, H.S. Genotype × site × silviculture interactions in radiata pine: Knowledge, working hypotheses and pointers for research. *N. Z. J. For. Sci.* **2017**, *47*, 6. [CrossRef]
19. Hewitt, A.E. *New Zealand Soil Classification*, 3rd ed.; Manaaki Whenua Press: Lincoln, New Zealand, 2010.
20. Soil Survey Staff. *Keys to Soil Taxonomy*, 13th ed.; National Resources Conservation Service, United States Department of Agriculture: Washington, DC, USA, 2022. Available online: https://www.nrcs.usda.gov/resources/guides-and-instructions/keys-to-soil-taxonomy (accessed on 30 December 2025).
21. Rijkse, W.C. *Soils of Taupo Region: Interim Soil Maps and Legend*; Research Paper; New Zealand Soil Bureau District Office: Rotorua, New Zealand, 1986. [CrossRef]
22. Smaill, S.J.; Garrett, L.G.; Addison, S.L. Accelerator trial series in Pinus radiata stands in New Zealand: Trial establishment, site description and initial soil, forest floor and tree data. *Data Brief* **2023**, *47*, 108991. [CrossRef]
23. Vincent, T.G.; Dunstan, J.S. *Register of Commercial Seedlots Issued by the New Zealand Forest Service*; Forest Research Institute Bulletin No. 144; Forest Research Institute: Rotorua, New Zealand, 1989; pp. 1–155.
24. rapidlasso GmbH. *LAStools*; rapidlasso GmbH: Gilching, Germany, 2025. Available online: https://rapidlasso.com/LAStools (accessed on 30 December 2025).
25. Roussel, J.R.; Auty, D.; Coops, N.C.; Tompalski, P.; Goodbody, T.R.H.; Sánchez Meador, A.; Bourdon, J.F.; de Boissieu, F.; Achim, A. Lidr: R Package Anal. Airborne Laser Scanning (ALS) data. *Remote Sens. Environ.* **2020**, *251*, 112061. [CrossRef]
26. R Core Team. *R: A Language and Environment for Statistical Computing*; R Foundation for Statistical Computing: Vienna, Austria, 2022. Available online: http://www.r-project.org/ (accessed on 12 December 2025).
27. Kimberley, M.O.; Beets, P.N. National volume function for estimating total stem volume of Pinus radiata stands in New Zealand. *N. Z. J. For. Sci.* **2007**, *37*, 355–371.
28. Mortensen, N.G.; Heathfield, D.N.; Myllerup, L.; Landberg, L.; Rathmann, O. *Getting Started with WAsP 9*; Risø National Laboratory, Technical University of Denmark: Roskilde, Denmark, 2007.
29. Mortensen, N.G.; Bowen, A.J.; Antoniou, I. *WAsP Engineering 2001*; Risø National Laboratory, Technical University of Denmark: Roskilde, Denmark, 2001.
30. Frank, H.P.; Rathmann, O.; Mortensen, N.G.; Landberg, L. *The Numerical Wind Atlas: The KAMM/WAsP Method*; Risø National Laboratory: Roskilde, Denmark, 2001.
31. Astrup, P.; Larsen, S.E. *WAsP Engineering Flow Model for Wind over Land and Sea*; Risø National Laboratory: Roskilde, Denmark, 1999; Risø-R No. 1107(EN).
32. Manaaki Whenua—Landcare Research. *LCDB v5.0—Land Cover Database Version 5.0, Mainland New Zealand*; Land Resource Information System (LRIS): Lincoln, New Zealand, 2020. Available online: https://lris.scinfo.org.nz/ (accessed on 27 August 2025).
33. European Environment Agency. *CORINE Land Cover (CLC)—Pan-European Land Cover Data for 1990–2018*; European Environment Agency: Copenhagen, Denmark, 2019.
34. Dörenkämper, M.; Olsen, B.T.; Witha, B.; Hahmann, A.N.; Davis, N.N.; Barcons, J.; Ezber, Y.; García-Bustamante, E.; González-Rouco, J.F.; Navarro, J.; et al. The making of the new european wind atlas–part 2: Production and evaluation. *Geosci. Model Dev.* **2020**, *13*, 5079–5102. [CrossRef]
35. Quine, C.P.; Gardiner, B.A.; Moore, J. Wind disturbance in forests: The process of wind-created gaps, tree overturning, and stem breakage. In *Plant Disturbance Ecology*; Elsevier: Amsterdam, The Netherlands, 2021; pp. 117–184.

36. Peterson, C.J.; Cannon, J.B. Modelling wind damage to southeastern U.S. trees: Effects of wind profile, gaps, neighborhood interactions, and wind direction. *Front. For. Glob. Change* **2021**, *4*, 719813. [CrossRef]
37. Cremer, K.W.; Borough, C.J.; McKinnell, F.H.; Carter, P.R. Effects of stocking and thinning on wind damage in plantations. *N. Z. J. For. Sci.* **1982**, *12*, 244–268.
38. Peltola, H.M. Mechanical stability of trees under static loads. *Am. J. Bot.* **2006**, *93*, 1501–1511. [CrossRef] [PubMed]
39. Duperat, M.; Gardiner, B.; Ruel, J.-C. Effects of a selective thinning on wind loading in a naturally regenerated balsam fir stand. *For. Ecol. Manag.* **2022**, *505*, 119–878. [CrossRef]
40. Locatelli, T.; Gardiner, B.; Hale, S.; Nicoll, B. Fgr: R Version of the ForestGALES Wind Risk Model, R package version 1.0. Available online: https://www.forestresearch.gov.uk/tools-and-resources/fthr/forestgales/fgr-the-forestgales-r-package/ (accessed on 10 December 2025).
41. Gardiner, B.; Byrne, K.; Hale, S.; Kamimura, K.; Mitchell, S.J.; Peltola, H.; Ruel, J.-C. A review of mechanistic modelling of wind damage risk to forests. *Forestry* **2008**, *81*, 447–463. [CrossRef]
42. Nicoll, B.C.; Gardiner, B.A.; Rayner, B.; Peace, A.J. Anchorage of coniferous trees in relation to species, soil type, and rooting depth. *Can. J. For. Res.* **2006**, *36*, 1871–1883. [CrossRef]
43. Fourcaud, T.; Ji, J.N.; Zhang, Z.Q.; Stokes, A. Understanding the impact of root morphology on overturning mechanisms: A modelling approach. *Ann. Bot.* **2008**, *101*, 1267–1280. [CrossRef]
44. Bonnesoeur, V.; Constant, T.; Moulia, B.; Fournier, M. Forest trees filter chronic wind-signals to acclimate to high winds. *New Phytol.* **2016**, *210*, 850–860. [CrossRef]
45. Gardiner, B.; Berry, P.; Moulia, B. Wind impacts on plant growth, mechanics and damage. *Plant Sci.* **2016**, *245*, 94–118. [CrossRef]
46. Nicoll, B.C.; Connolly, T.; Gardiner, B.A. Changes in spruce growth and biomass allocation following thinning and guying treatments. *Forests* **2019**, *10*, 253. [CrossRef]
47. Rudnicki, M.; Mitchell, S.J.; Novak, M.D. Wind tunnel measurements of crown streamlining and drag relationships for several conifer species. *Can. J. For. Res.* **2004**, *34*, 666–676. [CrossRef]
48. Gibbs, J.N.; Greig, B.J.W. Survey of parkland trees after the Great Storm of 16 October 1987. *Arboric. J.* **1990**, *14*, 321–347. [CrossRef]
49. Halstead, K.; Gaulton, R.; Sanderson, R.; Suggitt, A.; Quine, C. Localised damage patterns to oak during severe UK storms in winter 2021. *For. Ecol. Manag.* **2024**, *562*, 121942. [CrossRef]
50. Vollsinger, S.; Mitchell, S.J.; Byrne, K.E.; Novak, M.D.; Rudnicki, M. Wind tunnel measurements of crown streamlining and drag relationships for several hardwood species. *Can. J. For. Res.* **2005**, *35*, 1238–1246. [CrossRef]
51. Silen, R.R.; Olson, D.L.; Weber, J.C. Genetic variation in susceptibility to windthrow in young Douglas-fir. *For. Ecol. Manag.* **1993**, *61*, 17–28. [CrossRef]
52. Patacca, M.; Lindner, M.; Lucas-Borja, M.E.; Cordonnier, T.; Fidej, G.; Gardiner, B.; Hauf, Y.; Jasinevičius, G.; Labonne, S.; Linkevičius, E.; et al. Significant increase in natural disturbance impacts on European forests since 1950. *Glob. Change Biol.* **2023**, *29*, 1359–1376. [CrossRef]
53. Quine, C.P.; Gardiner, B.A. Understanding how the interaction of wind and trees results in windthrow, stem breakage, and canopy gap formation. In *Plant Disturbance Ecology*; Elsevier: Amsterdam, The Netherlands, 2007; pp. 103–155.


**Disclaimer/Publisher's Note:** The statements, opinions and data contained in all publications are solely those of the individual author(s) and contributor(s) and not of MDPI and/or the editor(s). MDPI and/or the editor(s) disclaim responsibility for any injury to people or property resulting from any ideas, methods, instructions or products referred to in the content.